

Degenerate Zeeman ground states in the single-excitation regime

R. T. Sutherland^{1,*} and F. Robicheaux^{1,2,†}

¹*Department of Physics and Astronomy, Purdue University, West Lafayette, Indiana 47907, USA*

²*Purdue Quantum Center, Purdue University, West Lafayette, Indiana 47907, USA*

(Received 6 September 2017; published 20 November 2017)

We demonstrate the importance of considering correlations between degenerate Zeeman sublevels that develop in dense atomic ensembles. In order to do this, we develop a set of equations capable of simulating large numbers of atoms while still incorporating correlations between degenerate Zeeman sublevels. This set of equations is exact in the single-photon limit and may be interpreted as a generalization of the frequently used coupled-harmonic-oscillator equations. Using these equations, we demonstrate that in sufficiently dense systems, correlations between Zeeman sublevels can cause nontrivial differences in the photon-scattering line shape in arrays and clouds of atoms.

DOI: [10.1103/PhysRevA.96.053840](https://doi.org/10.1103/PhysRevA.96.053840)

I. INTRODUCTION

Since its inception [1], the collective optics of both ordered and disordered ensembles has been a vibrant field of study [2–38]. The low-excitation (single-photon) regime is of particular interest since, in this limit, exact computations of ensembles of thousands of $J_g = 0 \rightarrow J_e = 1$ atoms are possible [2–12, 18, 19, 21, 22, 39]. This allows theorists to accurately simulate large clouds and arrays of atoms [6, 9, 18, 19]. Unfortunately, this technique only approaches exactness when the transitions that are probed have this angular momentum structure [11]. References [5] and [31] are an example of such a system, where the absence of fine structure in ⁸⁸Sr leads to a singlet ground state. However, most experimental setups do not contain this type of atom. For example, in many well-known experiments, ⁸⁷Rb, which contains degenerate ground states because of its hyperfine structure, is the atom of choice [4, 6, 9, 40]. This makes the development of potentially important quantum correlations possible.

The difference between an ensemble of $J_g = 0$ and $J_g \neq 0$ atoms could reasonably be mistaken as trivial, but it fundamentally changes the nature of the system. For atoms with $J_g = 0$ and $J_e = 1$, no matter how large the cloud of atoms is, there is a single ground state: $|ggg \dots g\rangle$. Further, in the low-excitation regime, a calculation must contain $3N$ singly excited states or, when there is significant magnetic splitting, N singly excited states. This is not the case when $J_g \neq 0$ since the Hilbert space describing the set of ground states contains $(2J_g + 1)^N$ elements, and the set of singly excited states contains $N(2J_e + 1)(2J_g + 1)^{N-1}$ elements. This makes the exact simulation of large clouds unfeasible, even in the single-photon limit. As a result, one approach that has been used is to stochastically distribute a Zeeman ground state M_g to each atom and set the correlation operators equal to zero [6, 9, 11]; see Eq. (8) below. As has been noted in Refs. [6, 9], these calculations produce line shapes that are qualitatively different than those observed experimentally.

It is well understood that quantum correlations can play an important role in sufficiently dense many-body systems.

In various regimes, this is often dealt with by solving for a set of physically relevant operators. Simulations containing many degrees of freedom are then made possible by truncating the resulting hierarchy of equations, either by factorizing or dropping higher-order correlation operators, via a cumulant expansion or some physically meaningful, alternative argument [11, 19, 37, 41, 42]. The presence of degenerate Zeeman ground states introduces the potential for quantum correlations between different atoms and Zeeman states that are absent in the $J_g = 0$ case. When $J_g \neq 0$, i.e., there are multiply degenerate Zeeman ground states, the system behaves in a fundamentally quantum manner with correlations which, as will be shown below, change the optical properties of the system. It should be noted that this issue was originally addressed in Ref. [11] through the field theoretical derivation of a hierarchy of operators capable of addressing these correlations to all orders. This present work derives a set of physically equivalent, yet perhaps more intuitive, equations by examining and exploiting the properties of the master equation [Eq. (1)] in the low-excitation limit. Further, we illustrate the fundamental importance of addressing these correlations by showing how the qualitative photon-scattering line shape in two experimentally relevant systems strongly depends on the presence of quantum correlations.

Specifically, we will derive both the lower-order oscillator equations used in [6, 9, 11], followed by a generalized version of these equations. The latter of these sets of equations includes the correlations that occur when $J_g \neq 0$. Further, we will introduce an approximation to this generalized technique, which is capable of simulating systems with large values of N . We will then show that the two techniques give different photon-scattering line shapes in both atomic arrays and clouds. This indicates that in order to properly simulate clouds of $J_g \neq 0$ atoms, one must consider higher-order quantum correlations. Lastly, we compare our results to the experimental observations of Ref. [9].

II. THEORY

A. Master equation

This work considers an ensemble of atoms interacting, via the dipole moments of an arbitrary $J_g \rightarrow J_e$ transition, with

*sutherland11@llnl.gov

†robichf@purdue.edu

both a laser and the quantized electromagnetic field. Assuming the system is Markovian, we use the Lindblad form of the master equation for the reduced density matrix $\hat{\rho}(t)$ [43,44],

$$\begin{aligned} \frac{d\hat{\rho}(t)}{dt} = & -\frac{i}{\hbar}[H, \hat{\rho}(t)] \\ & + \Gamma \sum_j \sum_{M_g M_g'} \sum_q C_{M_g}^q C_{M_g'}^q \{ \sigma_{M_g q}^{j-} \hat{\rho}(t) \sigma_{M_g' q}^{j+} \\ & - \frac{1}{2} \delta_{M_g M_g'} [\sigma_{M_g q}^{j+} \sigma_{M_g' q}^{j-} \hat{\rho}(t) + \hat{\rho}(t) \sigma_{M_g q}^{j+} \sigma_{M_g' q}^{j-}] \} \\ & + \sum_{j \neq j'} \sum_{M_g M_g'} \sum_{qq'} C_{M_g}^q C_{M_g'}^{q'} \{ [g_{jj'}^{qq'}(\alpha_{jj'}) \\ & + g_{jj'}^{qq'}(-\alpha_{jj'})] \sigma_{M_g' q'}^{j'-} \hat{\rho}(t) \sigma_{M_g q}^{j+} \\ & - g_{jj'}^{qq'}(\alpha_{jj'}) \sigma_{M_g q}^{j+} \sigma_{M_g' q'}^{j'-} \hat{\rho}(t) \\ & - g_{jj'}^{qq'}(-\alpha_{jj'}) \hat{\rho}(t) \sigma_{M_g q}^{j+} \sigma_{M_g' q'}^{j'-} \}. \end{aligned} \quad (1)$$

Here, $C_{M_g}^q \equiv \langle J_e(M_g + q) | 1q; J_g M_g \rangle$ is a Clebsch-Gordan coefficient, $\sigma_{M_g q}^{j+} \equiv |e J_e(M_g + q)\rangle_j \langle g J_g M_g| = (\sigma_{M_g q}^{j-})^\dagger$, Γ is the single-atom decay rate, $\alpha_{jj'} \equiv k|\mathbf{r}_j - \mathbf{r}_{j'}|$, and $g_{jj'}^{qq'}(\alpha_{jj'})$ is the inelastic and elastic dipole-dipole Green's function,

$$\begin{aligned} g_{jj'}^{qq'}(\alpha_{jj'}) \equiv & \frac{3\Gamma e^{i\alpha_{jj'}}}{4\alpha_{jj'}} \left[i \{ (\hat{\mathbf{e}}_q^* \cdot \hat{\mathbf{n}}_{jj'}) (\hat{\mathbf{e}}_{q'} \cdot \hat{\mathbf{n}}_{jj'}) - \delta_{qq'} \} \right. \\ & \left. + \left(\frac{1}{\alpha_{jj'}} + \frac{i}{\alpha_{jj'}^2} \right) \{ \delta_{qq'} - 3(\hat{\mathbf{e}}_q^* \cdot \hat{\mathbf{n}}_{jj'}) (\hat{\mathbf{e}}_{q'} \cdot \hat{\mathbf{n}}_{jj'}) \} \right], \end{aligned} \quad (2)$$

where $\hat{\mathbf{n}}_{jj'} \equiv (\mathbf{r}_j - \mathbf{r}_{j'})/|\mathbf{r}_j - \mathbf{r}_{j'}|$, and $\hat{\mathbf{e}}_q$ represents the q th unit polarization vector. Using the rotating-wave approximation,

$$\begin{aligned} H = & -\hbar\Delta \sum_j \sum_{M_e} |e J_e M_e\rangle_j \langle e J_e M_e| \\ & + \frac{\mathcal{D}}{2} \sum_j \sum_{M_g} \sum_q C_{M_g}^q \{ (\hat{\mathbf{e}}_q^* \cdot \mathbf{E}_j) \sigma_{M_g q}^{j+} + \text{c.c.} \}, \end{aligned} \quad (3)$$

where Δ is the detuning of the laser, \mathcal{D} is the reduced dipole matrix element [45], and \mathbf{E}_j is the laser field for atom j .

B. Hierarchy of correlation functions

In order to simulate such highly correlated systems, in this section, we will derive a hierarchy of operator expectation values using Eq. (1). Note that a physically equivalent, field-theoretical set of equations is presented in Ref. [11]. Here, we calculate the time dependence of the expectation value of the $\sigma_{M_g q}^{j-}$ operators using the equation

$$\frac{d\langle \sigma_{M_g q}^{j-} \rangle}{dt} = \text{Tr} \left\{ \sigma_{M_g q}^{j-} \frac{d\hat{\rho}(t)}{dt} \right\}. \quad (4)$$

This gives

$$\begin{aligned} \frac{d\langle \sigma_{M_g q}^{j-} \rangle}{dt} = & (i\Delta - \Gamma/2) \langle \sigma_{M_g q}^{j-} \rangle \\ & - \frac{i\mathcal{D}}{2\hbar} \sum_{M_g'} \sum_{q'} (\hat{\mathbf{e}}_{q'}^* \cdot \mathbf{E}_j) C_{M_g'}^{q'} \\ & \times \{ \langle \sigma_{M_g q}^{j-} \sigma_{M_g' q'}^{j+} \rangle \delta_{(M_g+q)(M_g'+q')} - \langle \sigma_{M_g' q'}^{j+} \sigma_{M_g q}^{j-} \rangle \delta_{M_g M_g'} \} \\ & - \sum_{j'' \neq j} \sum_{M_g''} \sum_{q''} C_{M_g''}^{q''} C_{M_g}^{q'} g_{jj''}^{q'q''}(\alpha_{jj''}) \\ & \times \{ \langle \sigma_{M_g'' q''}^{j''-} \sigma_{M_g q}^{j-} \sigma_{M_g' q'}^{j+} \rangle \delta_{(M_g+q)(M_g''+q'')} \\ & - \langle \sigma_{M_g'' q''}^{j''-} \sigma_{M_g' q'}^{j+} \sigma_{M_g q}^{j-} \rangle \delta_{M_g M_g'} \}. \end{aligned} \quad (5)$$

For this system, it is useful to probe the low-intensity ($|E||\mathcal{D}| \ll \Gamma\hbar$) limit. This allows one to set terms $\propto \sigma_{M_g' q'}^{j+} \sigma_{M_g q}^{j-}$ equal to zero since these terms only project onto states with excited atoms. Further, we consider only the case where the system is *initially* in an uncorrelated mixed state. This may be simulated by stochastically assigning each atom a Zeeman ground state M_g^j and then averaging over many runs [6,11]. This allows us to make the approximation $\langle \sigma_{M_g' q'}^{j+} \sigma_{M_g q}^{j-} \rangle \rightarrow \delta_{M_g' M_g} \delta_{q' q} \delta_{M_g M_g^j}$ since the development of correlations between different M_g values, for states with only ground-state atoms, is increasingly slow in the low-intensity limit. Considering these approximations gives

$$\begin{aligned} \frac{d\langle \sigma_{M_g q}^{j-} \rangle}{dt} \simeq & (i\Delta - \Gamma/2) \langle \sigma_{M_g q}^{j-} \rangle - \frac{i\mathcal{D}}{2\hbar} (\hat{\mathbf{e}}_q^* \cdot \mathbf{E}_j) C_{M_g}^q \delta_{M_g M_g^j} \\ & - \sum_{j'' \neq j} \sum_{M_g''} \sum_{q''} C_{M_g''}^{q''} C_{M_g}^{q'} g_{jj''}^{q'q''}(\alpha_{jj''}) \\ & \times \{ \langle \sigma_{M_g'' q''}^{j''-} \sigma_{M_g q}^{j-} \sigma_{M_g' q'}^{j+} \rangle \delta_{(M_g+q)(M_g''+q'')} \}. \end{aligned} \quad (6)$$

In order to solve for the one-atom correlation operators, one must solve for the two-atom correlation operators, and then the three-atom correlation operators, etc. This produces a hierarchy of equations that grows exponentially with N . Because of this, the expectation values of the correlation functions are often factorized in the following way:

$$\begin{aligned} \langle \sigma_{M_g'' q''}^{j''-} \sigma_{M_g q}^{j-} \sigma_{M_g' q'}^{j+} \rangle & \simeq \langle \sigma_{M_g'' q''}^{j''-} \rangle \langle \sigma_{M_g q}^{j-} \sigma_{M_g' q'}^{j+} \rangle \\ & \simeq \langle \sigma_{M_g'' q''}^{j''-} \rangle \delta_{M_g M_g''} \delta_{M_g M_g'} \delta_{q' q''}, \end{aligned} \quad (7)$$

keeping in mind that we have stochastically assigned a value of M_g^j to each atom. This gives

$$\begin{aligned} \frac{d\langle \sigma_{M_g q}^{j-} \rangle}{dt} \simeq & (i\Delta - \Gamma/2) \langle \sigma_{M_g q}^{j-} \rangle - \frac{i\mathcal{D}}{2\hbar} (\hat{\mathbf{e}}_q^* \cdot \mathbf{E}_j) C_{M_g}^q \delta_{M_g M_g^j} \\ & - \sum_{j'' \neq j} \sum_{M_g''} \sum_{q''} C_{M_g''}^{q''} C_{M_g}^{q'} g_{jj''}^{q'q''}(\alpha_{jj''}) \langle \sigma_{M_g'' q''}^{j''-} \rangle \delta_{M_g M_g''}. \end{aligned} \quad (8)$$

The approximate equations above are the ones typically used [5,6,9,18,19] and are exact when $J_g = 0$ and $J_e = 1$ [9]. The factorized terms in Eq. (7) are often *highly* correlated for dense

systems, making this approximation inadequate. In fact, as will be demonstrated in Sec. III, their presence changes the system's photon scattering in nontrivial ways. A technique capable of addressing these correlations, while remaining computationally pragmatic, is required.

C. Reduced master equation

In this section, we develop a system of equations capable of addressing the correlations that emerge in Eq. (1), in the low-intensity limit. An alternate, yet physically equivalent set of equations is presented in Ref. [11]. First, we write the density matrix in the following way:

$$\hat{\rho}(t) = \sum_{e,e'} \sum_{m,n} c_{e,m;e',n}(t) |e,m\rangle \langle e',n|. \quad (9)$$

Here, e represents the number of excitations in a given state and m is an index that runs over all the states within that subspace. We assume that the system is initialized in the pure state $|0,g\rangle$ and subsequently driven by a low-intensity laser. In the low-intensity limit,

$$|c_{0,g;0,g}| \simeq 1 \gg |c_{1,m;0,g}| \gg |c_{1,m';1,n'}|. \quad (10)$$

We also note that the rate of population transfer is $\propto c_{1,m;1,n}\Gamma$, while the system approaches a quasisteady state at a rate $\propto \Gamma$. Therefore, we neglect the effects of population transfer, i.e., terms in Eq. (1), $\propto \sigma_{M_g q}^{j-} \hat{\rho}(t) \sigma_{M_g q'}^{j+}$. Considering this, Eq. (1) shows that the $c_{0,g;0,g}$ density matrix element only couples to the $c_{1,m;0,g}$ elements, as well as their complex conjugates. Also, to first order, the $c_{1,m;0,g}$ density matrix elements are only coupled to the $c_{0,g;0,g}$ as well as the $c_{1,n;0,g}$ elements. The relevant space of density matrix elements only couples to states with $\langle 0,g|$ as the column state; therefore, the rows and the columns of the density matrix are completely uncorrelated, allowing us to rewrite $\hat{\rho}(t)$ as

$$\hat{\rho}(t) \simeq \sum_{e,e'} \sum_{m,n} c_{e,m}(t) c_{e',n}^*(t) |e,m\rangle \langle e',n|, \quad (11)$$

dramatically reducing the number of independent complex numbers needed to describe the density matrix. Further, in the low-intensity limit, the following properties are true:

$$\begin{aligned} |c_{0,g}(t)|^2 &\simeq 1, & c_{1,m}(t) c_{0,g}^*(t) &\simeq c_{1,m}(t), \\ |c_{1,m}(t) c_{0,g}^*(t)| &\gg |c_{1,m}(t) c_{1,k}^*(t)|, \\ |c_{1,m}(t) c_{1,k}^*(t)| &\gg O\left\{\left(\frac{D|E|}{2\hbar\Gamma}\right)^3\right\}. \end{aligned} \quad (12)$$

Considering the above approximations,

$$[c_{1,m}(t) c_{0,g}^*(t)][c_{0,g}(t) c_{1,n}^*(t)] \simeq c_{1,m}(t) c_{1,n}^*(t), \quad (13)$$

which allows one to construct any physical quantities $\propto c_{1m}(t) c_{1,n}^*(t)$, such as the photon-scattering rate, from the significantly smaller subspace of $c_{1,m}(t) c_{0,g}^*(t) \simeq c_{1,m}(t)$ density matrix elements. Note that the $c_{1,m}(t) c_{0,g}^*(t)$ terms will be labeled simply $c_{1,m}(t)$ from now on. Resultantly, we may solve for the system's dynamics from the $c_{1,m}(t)$ subspace, tracking only the operations on the left side of $\hat{\rho}(t)$.

This gives

$$\begin{aligned} \frac{dc_{1,m}(t)}{dt} &= (i\Delta - \Gamma/2)c_{1,m}(t) - \frac{iD}{2\hbar} (\hat{\mathbf{e}}_q^* \cdot \mathbf{E}_j) C_{M_g}^q \delta_{M_g M_g^j} \\ &- \sum_{n \neq m} \sum_{jj'} \sum_{M_g M_g^j} \sum_{qq'} C_{M_g}^q C_{M_g^j}^{q'} \\ &\times \{g_{jj'}^{qq'} (\alpha_{jj'}) \langle 1,n | \sigma_{M_g q}^{j+} \sigma_{M_g^j q'}^{j-} | 1,m \rangle c_{1,n}(t)\}. \end{aligned} \quad (14)$$

The amount of elements in this subspace is $N(2J_e + 1)(2J_g + 1)^{N-1}$, which is considerably less than the $4^N (J_e + J_g + 1)^{2N}$ elements in the full density matrix. This allows us to simulate clouds of significantly more atoms, while still including the relevant correlations present in systems with $J_g \neq 0$. An interesting feature of Eq. (14) is that it is equivalent to Eq. (8) for ensembles of $J_g = 0 \rightarrow J_e = 1$ atoms. For this angular momentum structure, both approaches are exact in the low-intensity regime and are equivalent to the coupled-harmonic-oscillator approach typically used in the literature [2–12,18,19,21,22,39]. This indicates that Eq. (14) may be viewed as a generalization to these equations.

Equation (14) approaches exactness in the limit where the system scatters a single real photon. This is shown in Fig. 1. Here, we compare calculations of the photon-scattering rate γ for individual configurations of dense clouds of four $J_g = 1/2$, $J_e = 1/2$ atoms driven by a plane-wave laser. In this figure, it is shown that for larger Rabi frequencies, the photon-scattering rate obtained using Eq. (1) yields different results than Eq. (14). However, for lower-intensity lasers, the two calculations are equivalent. Figure 1 also demonstrates that simulations using Eqs. (8) and (14) produce different photon-scattering rates, even at low laser intensities. Note that the results from Eq. (14) approach the exact result [i.e., Eq. (1)], while Eq. (8) does not. Equation (14) has the capacity to simulate much larger ensembles than Eq. (1). This is demonstrated in Fig. 2, where γ for a cloud of 16 atoms is calculated. Simulations with this many atoms are not possible when using Eq. (1) since the number of elements in the density matrix is more than 10^{13} times larger than the number required to use Eq. (14).

D. First-order correlations

While Eq. (14) allows one to simulate clouds containing significantly more atoms than Eq. (1) does, its computational capacity falls short of the ability to simulate clouds containing hundreds of atoms. Since this regime is that of recent experiments [6,9], an algorithm that can both simulate hundreds of atoms and still keep the *most relevant* correlations is needed. In order to accomplish this, we truncate the set of terms that Eq. (14) spans.

First, the system is stochastically assigned the pure state with zero excitations, labeled $|0,g\rangle$. Here, and in the rest of this work, we assume a \hat{z} polarized laser. Upon a given initialization, the set of $c_{1,n} |1,n\rangle \langle 0,g|$ obtained through all permutations of the following operation is kept:

$$\sigma_{M_g^j q'}^{j+} \sigma_{M_g^j q}^{j-} \sigma_{M_g 0}^{j+} |0,g\rangle, \quad (15)$$

while all other terms are set to zero. In other words, we keep the terms that are obtainable through an absorption of a single \hat{z} polarized photon from the laser, as well as the states obtainable

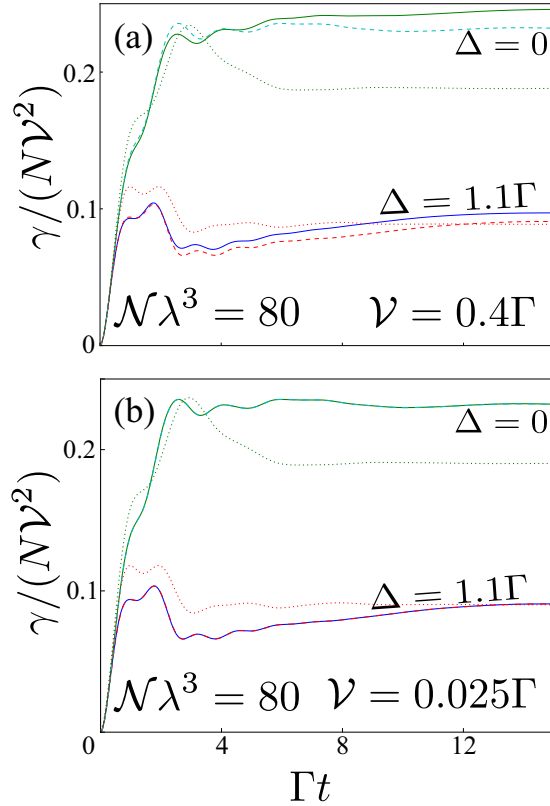


FIG. 1. Comparison between the photon-scattering rates γ , calculated using Eq. (1) (solid lines), Eq. (8) (dotted lines), and the approximate Eq. (14) (dashed lines), for a single, dense, randomly distributed, Gaussian ensemble of four atoms. (a) Comparison of the photon-scattering rate for systems being driven with a laser such that $\mathcal{V} = 0.4\Gamma$, where $\mathcal{V} \equiv |E_z||\mathcal{D}|/2\hbar$. This is shown for both on-resonance light, $\Delta = 0$, and blue-detuned light, $\Delta = 1.1\Gamma$. (b) The same comparison for $\mathcal{V} = 0.025\Gamma$. This demonstrates that the two calculations give the same answer as $\mathcal{V}/\Gamma \rightarrow 0$. Note that the discrepancies between calculations using Eq. (8) and using Eq. (14) do not diminish with laser intensity.

through the exchange of one photon between atoms. This is useful because the size of the relevant space scales $\propto N^2$ as opposed to exponentially. Unlike Eq. (14), this algorithm's scaling with N is independent of the level structure of the system, allowing for the simulation of large clouds of atoms with complex angular momentum structures. The following sections demonstrate that these approximations yield accurate results in many relevant systems.

III. RESULTS

A. Photon scattering in an array of atoms

The collective nature of dipole-dipole interactions in a one-dimensional array has been shown to produce nontrivial radiative properties [9,19,30,39]. For this system, we show the importance of correlations between degenerate Zeeman ground states by demonstrating their effect on the photon scattering of an array containing $J_g = 1/2 \rightarrow J_e = 1/2$ atoms. Here the array is aligned along the \hat{y} direction, while the laser is a plane wave propagating along the \hat{x} direction and polarized in the \hat{z} direction. All of the results here are for an initially

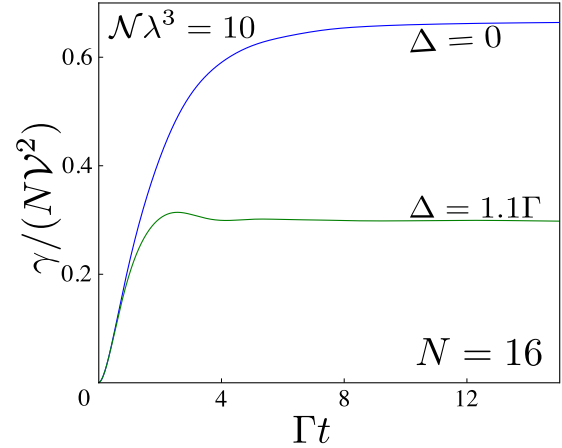


FIG. 2. The photon scattering γ for a single stochastically generated cloud of 16 $J_g = 1/2 \rightarrow J_e = 1/2$ atoms vs time.

uncorrelated mixture of Zeeman ground states, where every value of M_g has an equal probability. For all the calculations shown, this is simulated by stochastically averaging over 320 runs where every atom is assigned a random value of M_g .

The results from Eq. (14) are compared with the results from both Eqs. (8) and (15). This is, to some extent, a good quantification of the importance of correlations in the photon-scattering process. Equation (14) contains correlations between Zeeman states to all orders, Eq. (15) only includes the correlations resulting from a single virtual photon exchange between states, while Eq. (8) contains none of these correlations.

Figure 3 compares the steady-state photon scattering rate γ versus detuning Δ for an array of atoms using Eqs. (8), (15), and (14). In the figure, it is seen that for array spacings of 0.6λ , the photon-scattering line shape is equivalent using

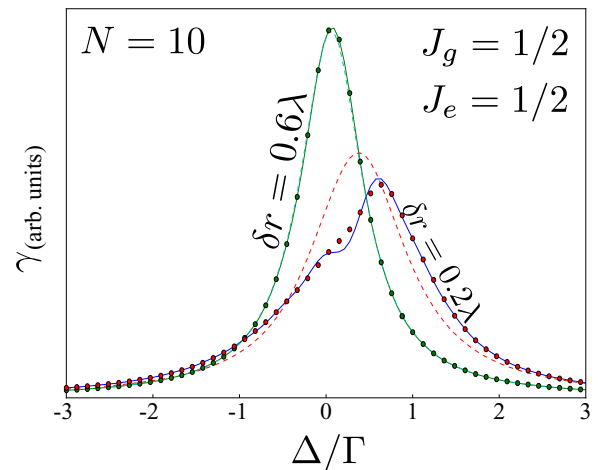


FIG. 3. The photon scattering γ vs Δ for 1D arrays of ten $J_g = 1/2 \rightarrow J_e = 1/2$ atoms. The line shape is calculated using Eq. (8) (dotted lines), Eq. (15) (solid circles), and Eq. (14) (solid lines) for various array spacings δr . Note that for larger values of δr , the two calculations agree well, indicating that correlations between degenerate Zeeman states are less important. However, for smaller array spacings, the effects of correlations on the photon scattering are clearly seen.

all three methods. This indicates that in this regime, higher-order correlations do not play a significant role in the system. Since the rate of virtual photon exchanges between states is $\propto 1/\delta r^3$, for smaller array spacings, correlations develop and the photon-scattering line shapes given by the three methods become qualitatively different. This is shown in Fig. 3, where for array spacings of $\delta r = 0.2\lambda$, the line shape calculated using Eq. (8) is still a Lorentzian structure, while the line shapes calculated using both Eqs. (14) and (15) have deviated from a Lorentzian shape, clearly forming double-peaked structures. The figure demonstrates that for this value of δr , many of the differences between Eqs. (8) and (14) can be explained by the first-order correlations given by Eq. (15) since two the calculations produce similar results. For even smaller array spacings, however, the results between all three calculations qualitatively differ. This is indicative of the fact that here, even higher-order correlations need to be included.

B. Photon scattering in a cloud of atoms

In this section, we calculate the line shape of the scattered radiation from a Gaussian cloud, with an average density $\mathcal{N} = \frac{N}{\sigma_x \sigma_y \sigma_z (4\pi)^{3/2}}$ and a distribution

$$\rho(\mathbf{r}) = \frac{N}{\sigma_x \sigma_y \sigma_z (2\pi)^{3/2}} \exp\left(-\left\{\frac{x^2}{2\sigma_x^2} + \frac{y^2}{2\sigma_y^2} + \frac{z^2}{2\sigma_z^2}\right\}\right), \quad (16)$$

driven by a plane-wave laser polarized in the \hat{z} direction. This system is of particular interest due to recent experiments on cold clouds of ^{87}Rb [6,9]. ^{87}Rb has two hyperfine ground states: ($5S_{1/2} F = 1$) and ($5S_{1/2} F = 2$). In these two experiments, the atoms are optically pumped into the ($5S_{1/2} F = 2$) ground state, and the closed transition to the ($5P_{3/2} F = 3$) excited state is probed. Presently, we demonstrate that such correlations make nontrivial differences in the optical properties of clouds. We should note that this section is incomplete with respect to the task of simulating the experimental results of Refs. [6,9] since it assumes, among other things, that the initial ground state is a completely uncorrelated mixture of Zeeman sublevels. However, it does demonstrate that these correlations play a vital role in understanding the line shape of a cloud. All of the results here are for an initially uncorrelated mixture of Zeeman ground states, where every value of M_g has an equal probability of being populated. For all the calculations shown, this is simulated by stochastically averaging over $6000/N$ runs where every atom is assigned a random position and value of M_g .

To start, Fig. 4 shows the importance of correlations for spherically symmetric clouds of ten $J_g = 1/2 \rightarrow J_e = 1/2$ atoms. Here all three calculations have been compared for different values of $\mathcal{N}\lambda^3$. Again, one can see that Eq. (8) is insufficient to describe the photon scattering of the system. While Eq. (14) allows for the simulation of clouds of atoms that were previously unreachable, experimental relevance still requires significantly more atoms. Fortunately, Fig. 4 shows that for values of $\mathcal{N}\lambda^3 < 40$, which are relevant to Refs. [6,9], only first-order correlations are needed to obtain reasonably good agreement with Eq. (14). This shows that for these densities, keeping only the first-order correlations is sufficient.

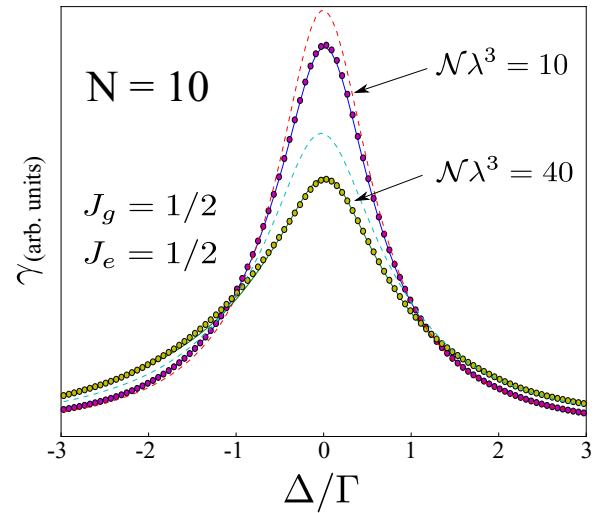


FIG. 4. The photon scattering for spherically symmetric Gaussian clouds of ten $J_g = 1/2 \rightarrow J_e = 1/2$ atoms vs detuning Δ for various densities \mathcal{N} . The importance of correlations between degenerate Zeeman ground states is shown by comparing Eq. (14) (solid lines), Eq. (15) (solid circles), and Eq. (8) (dotted lines). Note that the figure shows reasonable agreement between the results of Eqs. (14) and (15). This shows that for the values of \mathcal{N} shown, most of the relevant physics is described by first-order correlations.

Understanding the utility of keeping only the first-order correlations, we may apply our calculations to systems of experimental interest, i.e., atoms with $F_g = 2 \rightarrow F_e = 3$. In Fig. 5, we compare the photon-scattering line shape of a spherically symmetric cloud of 80 atoms using both Eq. (8), which includes no correlations, and the calculations keeping the first-order correlations; see Eq. (15). The presence of first-order correlations broadens the line shape to a nontrivial degree, suppressing the on-resonant scattering in particular. This again indicates the importance of correlations between Zeeman states upon calculating the line shape.

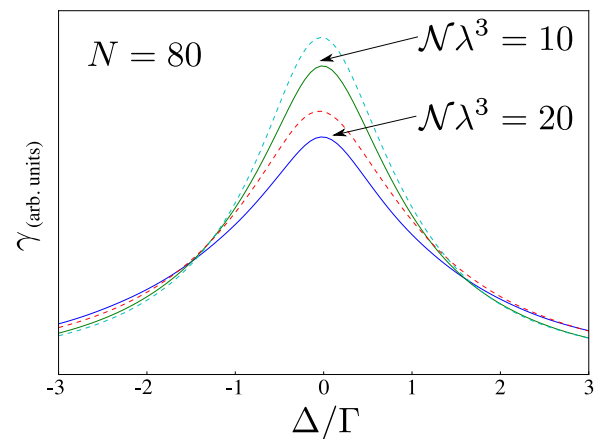


FIG. 5. The photon scattering for a spherically symmetric Gaussian cloud of 80 $J_g = 2 \rightarrow J_e = 3$ atoms. The dotted line corresponds to the results obtained using Eq. (8), which includes no Zeeman correlations, while the solid line is the calculation that includes the first-order correlations, given by Eq. (15).

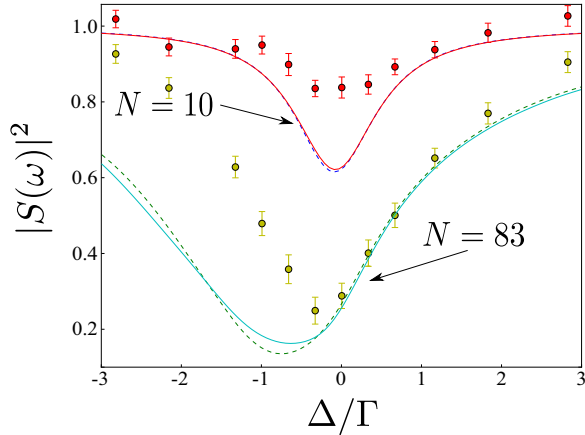


FIG. 6. $|S(\omega)|^2$, where $S(\omega)$ is the transfer function defined in the text, vs laser detuning Δ . The dotted line corresponds to the results obtained using Eq. (8), which includes no Zeeman correlations, while the solid line is the calculation that includes the first-order correlations, given by Eq. (15). The solid circles correspond to the experimental data originally reported in Ref. [9] and the calculations are conducted for these experimental specifications, as described in the text.

Reference [9] reports the coherent light transported through a cloud of atoms. They observe the transfer function,

$$S(\omega) = \frac{(\mathbf{E}_l + \mathbf{E}_s) \cdot \hat{\mathbf{z}}}{\mathbf{E}_l \cdot \hat{\mathbf{z}}} = 1 + \frac{\mathbf{E}_s \cdot \hat{\mathbf{z}}}{\mathbf{E}_l \cdot \hat{\mathbf{z}}}, \quad (17)$$

which is essentially a quantification of the interference between the electric field from the laser, \mathbf{E}_l , and the electric field scattered off of the atoms, \mathbf{E}_s , at the position of the detector. In Fig. 6, we compare the results from both Eq. (8) and the calculations that keep the first-order correlations in Eq. (14). This simulation uses the experimental parameters given in Ref. [9]. The cloud now has a fixed size, i.e., $\sigma_x = 1.5\lambda$, $\sigma_y = \sigma_z = 0.25\lambda$, which for the clouds of 10 and 83 atoms shown give values of $\lambda^3\mathcal{N} \simeq 2.4$ and $\lambda^3\mathcal{N} \simeq 19.9$, respectively. Unlike the previous simulations given above, the probe beam is now a linearly polarized Gaussian laser propagating in the $\hat{\mathbf{x}}$ direction, with an amplitude

$$E_{l,z}(\mathbf{r}) = \frac{E_0}{1 + i\frac{x}{x_R}} \exp\left[ik\frac{y^2 + z^2}{2q(x)}\right] \exp[ikx], \quad (18)$$

where $\frac{1}{q(x)} = \frac{1}{R(x)} + \frac{2i}{kw^2(x)}$, $x_R = kw^2/2$ is the Rayleigh length, $w(x) = w\sqrt{1 + x^2/x_R^2}$, E_0 is the field amplitude, and $R(x) = x + x_R^2/x$, where $w = 1.54\lambda$ is the waist of the laser. When comparing with the experimental data, one can see that the inclusion of correlations between Zeeman states does not explain the difference between the observations and

the calculations. While, similar to experimental observations, the calculations that include Zeeman correlations have a significantly smaller redshift than the results obtained using Eq. (8), the calculated line shape is still non-Lorentzian. This differs from experiment, where the key qualitative experimental observation is that the line shape is Lorentzian [9]. This could indicate that the assumption of an initial, completely uncorrelated mixture of Zeeman states is incorrect.

IV. CONCLUSION

In this work, it is demonstrated that in certain atomic systems, correlations between degenerate Zeeman ground states can have an important effect on the scattered light. This is first shown for one-dimensional (1D) arrays of atoms, where such correlations qualitatively change the photon-scattering line shape of a closely spaced array. It is also shown that for Gaussian clouds of multilevel atoms, the photon-scattering rate can be nontrivially changed by these correlations.

In order to simulate these regimes, we developed a set of equations capable of accurately simulating large ensembles of atoms coupled to the electromagnetic field, compared to the full master equation. For $J_g = 0$ atoms, this system is identical to the coupled-harmonic-oscillator equations commonly used in the literature, allowing Eq. (14) to be interpreted as a generalization of this approach. While this set of equations is capable of probing different regimes (see Fig. 3), it falls short of the capacity to simulate the large ensembles of atoms present in many experiments. Because of this, an approximation capable of simulating ensembles of the order of hundreds of atoms is developed; see Eq. (14). It is then demonstrated that in many systems, this approximation gives nearly identical results to Eq. (14), indicating its potential utility in reproducing experimental results in the future. Thus far, the effects of nondegenerate Zeeman structures have remained largely unexplored. In many cases, such atoms are often replaced by two-level atoms with modified dipole-dipole interactions. This work demonstrates that this approach is often inadequate since more complicated angular momentum structures result in correlations that produce rich physics and many systems cannot be understood unless this is explicitly considered.

ACKNOWLEDGMENTS

The authors would like to thank Janne Ruostekoski and Antoine Browaeys for informative conversations and data. This material is based upon work supported by the National Science Foundation under Grant No. 1404419-PHY. This research was supported in part through computational resources provided by Information Technology at Purdue University, West Lafayette, Indiana.

[1] R. H. Dicke, *Phys. Rev.* **93**, 99 (1954).

[2] M.-T. Rouabah, M. Samoylova, R. Bachelard, P. W. Courteille, R. Kaiser, and N. Piovella, *J. Opt. Soc. Am. A* **31**, 1031 (2014).

[3] T. Bienaimé, N. Piovella, and R. Kaiser, *Phys. Rev. Lett.* **108**, 123602 (2012).

[4] W. Guerin, M. O. Araújo, and R. Kaiser, *Phys. Rev. Lett.* **116**, 083601 (2016).

- [5] S. L. Bromley, B. Zhu, M. Bishof, X. Zhang, T. Bothwell, J. Schachenmayer, T. L. Nicholson, R. Kaiser, S. F. Yelin, M. D. Lukin, A. M. Rey, and J. Ye, *Nat. Commun.* **7**, 11039 (2016).
- [6] J. Pellegrino, R. Bourgain, S. Jennewein, Y. R. P. Sortais, A. Browaeys, S. D. Jenkins, and J. Ruostekoski, *Phys. Rev. Lett.* **113**, 133602 (2014).
- [7] J. Javanainen, J. Ruostekoski, Y. Li, and S.-M. Yoo, *Phys. Rev. Lett.* **112**, 113603 (2014).
- [8] G. Facchinetti, S. D. Jenkins, and J. Ruostekoski, *Phys. Rev. Lett.* **117**, 243601 (2016).
- [9] S. Jennewein, M. Besbes, N. J. Schilder, S. D. Jenkins, C. Sauvan, J. Ruostekoski, J.-J. Greffet, Y. R. P. Sortais, and A. Browaeys, *Phys. Rev. Lett.* **116**, 233601 (2016).
- [10] S. D. Jenkins, J. Ruostekoski, J. Javanainen, S. Jennewein, R. Bourgain, J. Pellegrino, Y. R. P. Sortais, and A. Browaeys, *Phys. Rev. A* **94**, 023842 (2016).
- [11] M. D. Lee, S. D. Jenkins, and J. Ruostekoski, *Phys. Rev. A* **93**, 063803 (2016).
- [12] A. A. Svidzinsky, J.-T. Chang, and M. O. Scully, *Phys. Rev. A* **81**, 053821 (2010).
- [13] H. Harde and D. Grischkowsky, *J. Opt. Soc. Am. B* **8**, 1642 (1991).
- [14] M. Gross and S. Haroche, *Phys. Rep.* **93**, 301 (1982).
- [15] M. Gross, C. Fabre, P. Pillet, and S. Haroche, *Phys. Rev. Lett.* **36**, 1035 (1976).
- [16] M. Gross, J. M. Raimond, and S. Haroche, *Phys. Rev. Lett.* **40**, 1711 (1978).
- [17] N. E. Rehler and J. H. Eberly, *Phys. Rev. A* **3**, 1735 (1971).
- [18] R. T. Sutherland and F. Robicheaux, *Phys. Rev. A* **93**, 023407 (2016).
- [19] R. T. Sutherland and F. Robicheaux, *Phys. Rev. A* **94**, 013847 (2016).
- [20] R. T. Sutherland and F. Robicheaux, *Phys. Rev. A* **95**, 033839 (2017).
- [21] R. J. Bettles, S. A. Gardiner, and C. S. Adams, *Phys. Rev. A* **92**, 063822 (2015).
- [22] R. J. Bettles, S. A. Gardiner, and C. S. Adams, *Phys. Rev. Lett.* **116**, 103602 (2016).
- [23] M. O. Scully, E. S. Fry, C. H. Raymond Ooi, and K. Wódkiewicz, *Phys. Rev. Lett.* **96**, 010501 (2006).
- [24] M. Scully, *Laser Phys.* **17**, 635 (2007).
- [25] M. O. Scully, *Phys. Rev. Lett.* **102**, 143601 (2009).
- [26] M. O. Scully, *Phys. Rev. Lett.* **115**, 243602 (2015).
- [27] H. Bender, C. Stehle, S. Slama, R. Kaiser, N. Piovella, C. Zimmermann, and P. W. Courteille, *Phys. Rev. A* **82**, 011404 (2010).
- [28] P. W. Courteille, S. Bux, E. Lucioni, K. Lauber, T. Bienaime, R. Kaiser, and N. Piovella, *Eur. Phys. J. D* **58**, 69 (2010).
- [29] H. H. Jen, M.-S. Chang, and Y.-C. Chen, *Phys. Rev. A* **94**, 013803 (2016).
- [30] H. Jen, *Phys. Rev. A* **96**, 023814 (2017).
- [31] T. Ido, T. H. Loftus, M. M. Boyd, A. D. Ludlow, K. W. Holman, and J. Ye, *Phys. Rev. Lett.* **94**, 153001 (2005).
- [32] J. Ruostekoski and J. Javanainen, *Phys. Rev. A* **55**, 513 (1997).
- [33] J. Hernández, L. Noordam, and F. Robicheaux, *J. Phys. Chem. B* **109**, 15808 (2005).
- [34] A. S. Kuraptsev and I. M. Sokolov, *Phys. Rev. A* **90**, 012511 (2014).
- [35] R. Monshouwer, M. Abrahamsson, F. van Mourik, and R. van Grondelle, *J. Phys. Chem. B* **101**, 7241 (1997).
- [36] M. A. Palacios, F. L. de Weerd, J. A. Ihalainen, R. van Grondelle, and H. van Amerongen, *J. Phys. Chem. B* **106**, 5782 (2002).
- [37] B. Zhu, J. Schachenmayer, M. Xu, F. Herrera, J. G. Restrepo, M. J. Holland, and A. M. Rey, *New J. Phys.* **17**, 083063 (2015).
- [38] B. Zhu, J. Cooper, J. Ye, and A. M. Rey, *Phys. Rev. A* **94**, 023612 (2016).
- [39] R. J. Bettles, S. A. Gardiner, and C. S. Adams, *Phys. Rev. A* **94**, 043844 (2016).
- [40] S. J. Roof, K. J. Kemp, M. D. Havey, and I. M. Sokolov, *Phys. Rev. Lett.* **117**, 073003 (2016).
- [41] R. Kubo, *J. Phys. Soc. Jpn.* **17**, 1100 (1962).
- [42] D. Meiser, J. Ye, D. R. Carlson, and M. J. Holland, *Phys. Rev. Lett.* **102**, 163601 (2009).
- [43] D. F. V. James, *Phys. Rev. A* **47**, 1336 (1993).
- [44] G. S. Agarwal and A. K. Patnaik, *Phys. Rev. A* **63**, 043805 (2001).
- [45] R. Shankar, *Principles of Quantum Mechanics* (Springer Science & Business Media, New York, 2012).